Supplemental Data

DSAS-6 Organizes a Tube-like Centriole Precursor, and Its Absence Suggests Modularity in Centriole Assembly

Ana Rodrigues-Martins, Mónica Bettencourt-Dias, Maria Riparbelli, Cláudia Ferreira, Inês Ferreira, Giuliano Callaini, and David M. Glover

Supplemental Experimental Procedures

Flies and Husbandry

Two *DSAS-6* mutant alleles, *PBac{PB}CG15524[c02901]* [S1] (an insertion in the ORF) and *Df(3R)Excel6213,P{xp-u}* [S1] (a deficiency that uncovers the gene), were acquired from Bloomington and used in this study. All analysis was performed on hemizygous flies, and we refer to those flies as *DSAS-6* mutants in the text. *pUbq-GFP-PACT* flies were kindly provided by J. Raff [S2]. *pUbq-GFP-DSAS-6* and *pUASp-GFP-DSAS-6* transgenic flies were made by us (injected at http://www.thebestgene.com). *V32-gal4* flies were used as a driver for overexpression in female germ line (kindly provided by D. St Johnston). *OreR* stocks were used as wild-type. All flies were reared according to standard procedures and maintained at 25°C.

Constructs

pUbq-GFP-DSAS-6 and pUASp-GFP-DSAS-6 constructs were made with the gateway system from Invitrogen. The destination vectors pUbq-GFP and pUASp-GFP were kindly provided by R. Basto and the DRGC (http://dgrc.cgb.indiana.edu/), respectively.

RNAi and Transfections

Production of dsRNA and transfections were performed as described [S3, S4]. In brief, cells were transfected with 40 μg of dsRNA for GFP (control) and for DSAS-6. Cells were fixed 4 days afterwards, and the number of mitotic cells and spindle defects and the number of mitotic cells showing 0 centrosomes were scored as previously [S5]. Primers used for dsRNA production were DSAS-6F-*TAATACGACTCACTATAGGGAGATGTAGTGCGCATGCTGAAGGAC*; DSAS-6R-*TAATACGACTCACTATAGGGAGAGCTGCGCTGCTCGTTTATTTTG*; GFP-F-*TAATACGACTCACTATAGGGAGACTTCAGCCGCTACCCC*; GFP-R-*TAATACGACTCACTATAGGGAGATGTCGGGCAGCACG*; SPD2-F-*TAATACGACTCACTATAGGGAGACCTGACTTCTCCCTGGGCAACTAC*; and SPD2-R-*TAATACGACTCACTATAGGGAGATCAATGGCAGACAGGGACAGGA*.

Antibodies

We used the following antibodies: chicken anti-DSAS-6 (produced in our own lab, 1:1000); rat anti-α-tubulin-YL1/2 (Oxford Bioscences,1:50); rabbit anti-actin (Sigma, 1:2000); mouse anti-γ-tubulin-GTU88 (Sigma,1:25); rabbit anti-centrosomin (Cnn,1:300 [S4]); rabbit anti-DSAS-4 (1:500 [S6]); chicken anti-D-PLP (produced in our own lab 1:1000 [S7]); rabbit anti-SDP-2 (produced in our own lab, 1:500); mouse anti-GFP (Roche, 1:50); and rabbit anti-GFP (Abcam, 1:100). The secondary antibodies used (1:250 for imunofluorescence and 1:10,000 for western blot) to detect all antigens had minimal cross reactivity to other species and were conjugated with Rhodamine Redex, Peroxidase (Jackson Imunochemicals), FITC (SIGMA), or CY5 (Jackson Imunochemicals). For anti-DSAS-6 antibody

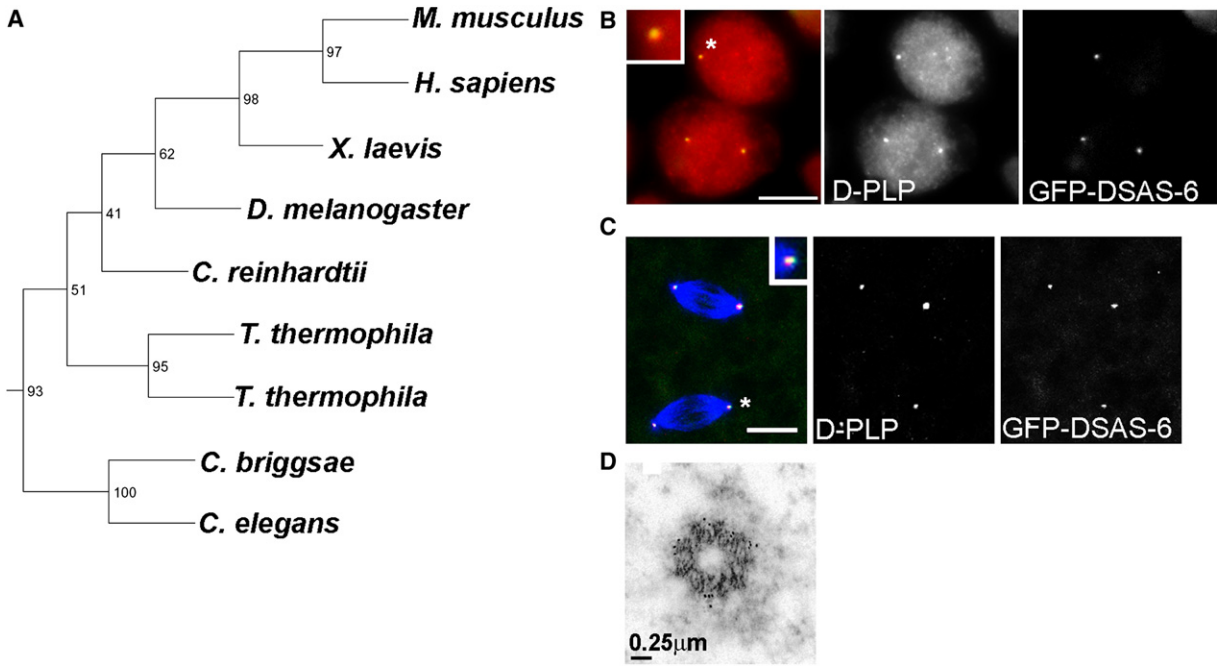

Figure S1. DSAS-6 Is the Only *Drosophila* Ortholog of the *C. elegans* and Human SAS-6 and Localizes to Centrioles

(A) Maximum likelihood tree of SAS-6 sequences. Labels on branches indicate bootstrap values in percentages. DSAS-6 is the only *Drosophila* ortholog of the *C. elegans* and human SAS-6.

(B and C) GFP-DSAS-6 colocalizes with D-PLP at the centrosomes in both (B) *Drosophila* S2 cells and (C) *Drosophila* embryos. D-PLP (red), GFP-DSAS-6 (green), α-tubulin (blue). Insets are 2× magnification of centrosome marked with an asterisk (D-PLP channel). Scale bar represents 10 μm.

(D) Immunoelectron microscopy of GFP-DSAS-6 in *Drosophila* spermatocyte centrioles suggests that this protein localizes to centrioles. Scale bar as indicated.

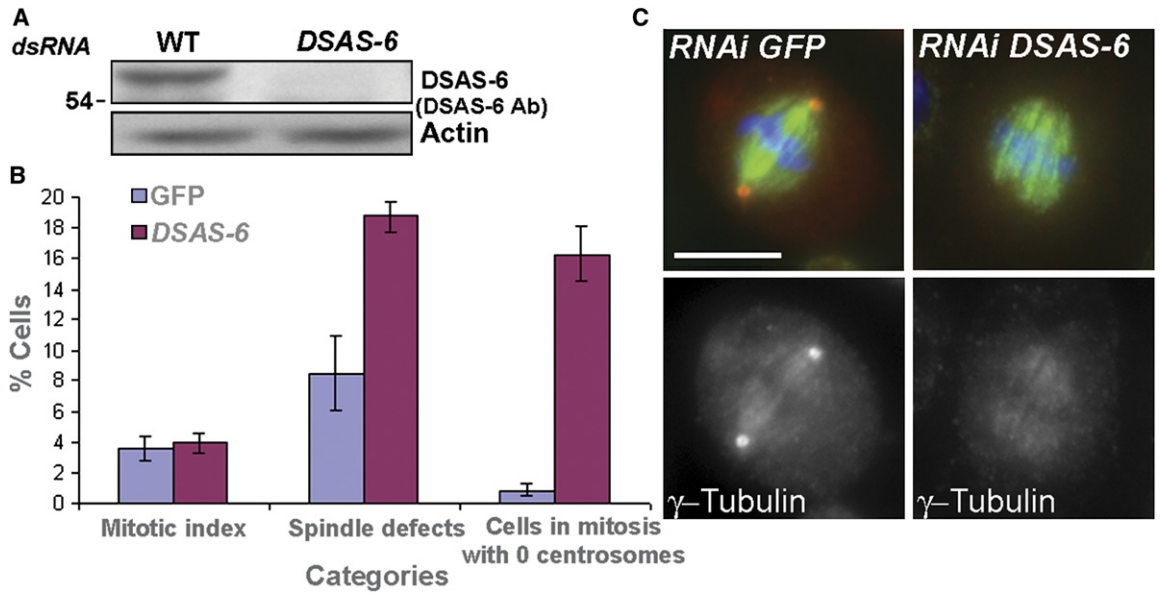

Figure S2. DSAS-6 Is Required for Centriole Duplication in S2 Cells

(A) Depletion of DSAS-6 after RNAi for 4 days in S2 cells.

(B and C) RNAi against DSAS-6 leads to an increase in spindle defects, which includes broad spindles, and an increase in the number of cells in mitosis with 0 centrosomes as defined in [S5] (counted by γ-tubulin staining). Note that the observed defects are similar to the ones we previously reported after SAK/PLK4 RNAi [S4], suggesting similar function. Almost complete depletion of centrosomes in the population is seen only after 12 days of RNAi for DSAS-6, because only then the existing pool of centrosomes is diluted with cell divisions [S7]. γ-tubulin (red), α-tubulin (green), DNA (blue). Three independent experiments were performed. Error bar indicates SEM. Scale bar represents 10 μm.

production, the whole DSAS-6 protein was expressed in *E. coli* from a modified pet23b (Novagen) gateway vector, purified, and injected into chickens (Harlan Sera, UK). For anti-DSPD-2 antibody production, a recombinant protein fragment (amino acid residues 375–695) was expressed in the same system as above, purified, and injected into rabbits (Harlan Sera, UK). The primers used to make the recombinant constructs were DSAS-6-F *GGGGACAAGTTTGTACAAAAAAGCAGGCTTCGAAGGAGATAGAACCATGTGGCCTCCAGGGAGCGAGGATA*; DSAS-6-R-*GGGGACCACTTTGTACAAGAAAGCTGGGTCCTATCGCCGATTTTCTTTGCCCGTGGGTAT*; DSPD-2-375F-*GGGGACAAGTTTGTACAAAAAAGCAGGCTTCAGGAATGGTCTGGCAGCCAAAGAGA*; and DSPD-2-375R-*GGGGACCACTTTGTACAAGAAAGCTGGGTCTTAATCGCGATGACTGAACTCACTAGA*.

Western Blot

Protein extracts from tissue cultured cells, larval brains, embryos, eggs, and ovaries were prepared after homogenization in SDS-PAGE sample buffer, boiling for 10 min, and spinning at high speed to clear the lysate. 30 brains were used per lane.

Cell/Testis/Brain Staining

Tissue culture cells were permeabilized and stained as previously [S4]. Testes from pharate adults were dissected in testes buffer (183 mM KCl, 47 mM NaCl, 1 mM EDTA, 10 mM Tris-HCl [pH 6.8]), fixed in methanol and acetone, and stained as described in [S8]. For live images of testes by phase microscopy, testes were dissected in 0.7% NaCl. For γ-tubulin, D-PLP, and α-tubulin staining, larval brains were prepared and treated as previously [S9]. Brain squashes were carried out as previously [S10]. After being frozen in liquid nitrogen, slides were fixed in ice-cold methanol for 10 min. They were then rehydrated in PBS + 0.1% Triton for 10 min; immunostaining was then performed for phospho-histone H3, DAPI, and D-PLP. The mitotic index was determined as the ratio of phospho-histone H3-positive (mitotic cells) per total (DAPI-stained) cells.

Embryos/Eggs/Ovaries and 14 Stage Oocytes Staining

Embryos/eggs from 4- to 5-day-old flies were collected at 25°C on small agar plates, dechorionated in a freshly made 50% bleach solution, and washed with distilled water. The Viteline membrane was removed by shaking vigorously in a 50% solution of methanol and heptane for 3 min. Eggs were fixed and stained as described before [S11]. Ovaries from 2- to 3-day-old well-fed females were dissected in PBS and the tips of the ovaries were teased open. Gonads were fixed for 30 min in 4% formaldehyde in PBS; staining was performed as described [S12]. To stain stage 14 oocytes, ovaries from 2- to 3-day-old well-fed females were dissected in absolute methanol and transferred to a 14 ml plastic tube containing 3 ml of fresh methanol. About 12–24 single ovaries were prepared in this way and then sonicated with a water bath sonicator (Branson 2000) for 5–10 cycles of 2 s each, until the majority of the 14 stage oocytes had lost their chorion. Staining of 14 stage oocytes was then performed as described [S13].

Imaging

Testes, brains, embryos/eggs, ovaries, and 14 stage oocytes were examined with either an MRC-1024 BioRad confocal scanning head mounted on an Optiphot microscope (Nikon) or a Leica SP-2 confocal scanning head. Images shown are the maximum-intensity projections of optical sections acquired at 0.5 μm. Number of centrioles, centriole length, and spatial position of centrioles within centrosomes was measured in 16 cells, G2 cysts. The following categories were used for the length of centrioles: smaller than 0.5 μm, 0.5–1 μm, and bigger than 1 μm. To calculate the perimeter of the cysts, images of 16-cell cysts were exported to the image analysis software, ImageJ, where we used the option "Measure Perimeter." A threshold of 1860 px was used to define "early" and "late" cysts. Phase-contrast photographs were taken with a Nikon Coolix 990 digital camera on a Nikon Microphot-F X microscope. An axiovert 200M microscope and a Leica DMRA2 were used for observation and counting of tissue culture and brain squash preparations. Images on these microscopes were acquired with a Photometrics Cool SNAP HQ camera and the software Metamorph.

Transmission Electron Microscopy Analysis of Testes and Embryos

Testes were dissected in phosphate buffer, fixed in 4% paraformaldehyde (EM grade) in PBS for 15 min. Testes were then immersed in 2.5% glutaraldehyde in 0.1 M phosphate buffer (pH 7.2) for 2 hr at

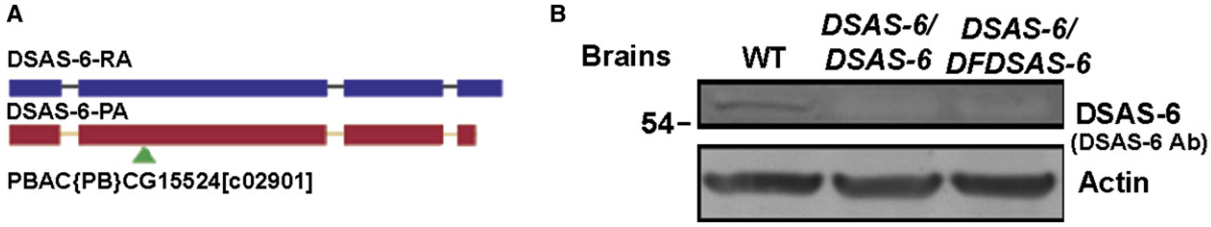

C

Genotype analysed	DSAS-6/DSAS-6 (Homozygotes)				DSAS-6/DFDSAS-6 (Hemizygotes)				pUbqGFP-DSAS-6; DSAS-6/DSAS-6 (Rescue)			
Stage (number of flies scored)	Pupae (n=974)	Adults (n=674)	Fertility		Pupae (n=929)	Adults (n=612)	Fertility		Pupae (n=500)	Adults (n=500)	Fertility	
Sex	M & F	M & F	M	F	M & F	M & F	M	F	M & F	M & F	M	F
Results observed (%) (Expected %)	28 (33)	0 (33)	N/A	N/A	33 (33)	0 (33)	N/A	N/A	33 (33)	33 (33)	100	100

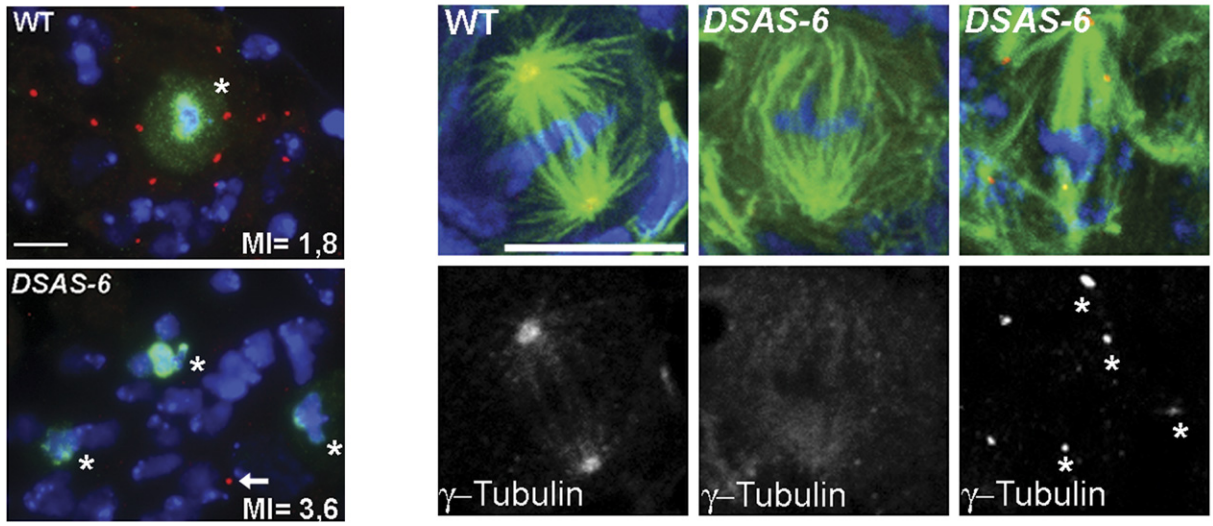

Figure S3. DSAS-6 Is Required for Eclosion and Centriole Duplication in *Drosophila*

(A) Schematic representation of the *DSAS-6* transcript (DSAS-6-RA) and DSAS-6 open reading frame (DSAS-6-PA) as assigned in FlyBase (*CG15524*) for the *Drosophila* ortholog of the *C. elegans SAS*-6. The green triangle marks the site of insertion of the transposon element PBac{PB}CG15524[c02901] in the second exon as assigned by Excelexis [S1].

(B) *DSAS-6* homozygous and hemizygous mutant brains show absence of DSAS-6 protein. 30 brains were used per lane because DSAS-6 is expressed in low levels like other centriolar proteins [S4, S6].

(C) *DSAS-6* mutant is genetically a null because both homozygous and hemizygous mutants have the same lethal phase (pharate adults). Deficiency *Df(3R)Exel6213*, named *DFDSAS-6*, uncovers the *DSAS-6* gene. N/A, nonapplicable. Because almost all *DSAS-6* mutants die as pharate adults, it is impossible to test fertility. Transgenic flies harboring one copy of *GFP-DSAS-6* under a polyubiquitin (pUbq) promoter rescue the *DSAS-6* mutant lethality and allow fertility.

(D) Brain squashes of *DSAS-6* mutants showed an increase in mitotic index (2×) and a decrease in centrosome number (16×) as shown by D-PLP staining. Arrow indicates centrosome. Asterisk indicates mitotic cells. D-PLP (red), phospho-histone-H3 (green), DNA (blue). A minimum of 6000 cells were counted in each of three independent experiments. Data shown are an average.

(E) The majority of the mitotic cells in *DSAS-6* mutant brains had no centrosomes (middle), whereas 18% showed smaller centrosomes (right). Among these, there were cells showing more than two small γ-tubulin foci (8% of the mitotic cells), suggestive of centriole splitting and perhaps smaller centrioles. Asterisk indicates centrosomes from the same cell. n = 100 mitotic cells. γ-tubulin (red), α-tubulin (green), DNA (blue). Scale bar represents 10 μm.

4°C. The testes were then washed three times for 30 min in phosphate buffer, postfixed with 1% OsO_4 for 1 hr at 4°C, washed once more in buffer, and then washed in distilled water. Samples were stained for 1 hr in uranyl acetate. They were washed again, dehydrated in a series of ethanols, and embedded in Epon-Araldite. After polymerization for 2 days at 60°C, the coverslips were removed from the resin after a short immersion in liquid nitrogen. Ultrathin serial sections were obtained with a LKB ultratome, stained with uranyl acetate and lead citrate, and observed and photographed with a Philips CM10 electron microscope at 80 kV. Wild-type and embryos/eggs overexpressing D-SAS-6 were collected for 2–3 hr on small agar plates at 24°C. Embryos/eggs were dechorionated in a 50% bleach

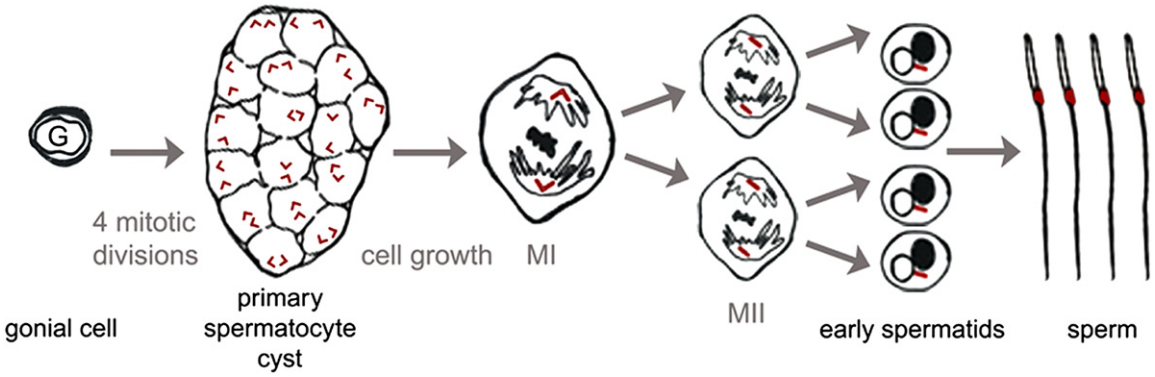

Figure S4. Spermatogenesis in *Drosophila*

During spermatogenesis, each stem cell division produces a gonial cell that undertakes four rounds of mitosis to produce a cyst of 16 primary spermatocytes. These are connected through 15 ring canals as result of incomplete cytokinesis. Each of these cells has four centrioles (red bars) and undertakes a prolonged G2 phase, where the cells and their centrioles grow substantially. Centrioles within the centrosome remain close together in a V-shape. During this phase, all centrioles within each cell migrate to the membrane and form a small cilium. Afterwards, they migrate again to a position closer to the nucleus, in preparation for meiosis. Meiotic divisions produce a cyst of 64 interconnected spermatids, each with one centriole. Early spermatids have a single nucleus (white sphere) and a mitochondrial derivative (Nebenkern, black sphere) of similar sizes. The spermatid centriole differentiates into a basal body to organize the flagellar axoneme of the sperm. From [S4].

solution and washed with distilled water. Dechorionated embryos/eggs were treated with 25% glutaraldehyde in PBS with an equal volume of heptane for 3 min. Embryos/eggs were then transferred for 30 min to 2.5% glutaraldehyde in PBS and the vitelline envelope was removed with tungsten needles. The devitellinized embryos/eggs were incubated overnight at 4°C in glutaraldehyde 2.5%. After rinsing in PBS, the samples were postfixed in 1% osmium tetroxide for 2 hr at 4°C and dehydrated in a graded series of alcohols, embedded in an Epon-Araldite mixture, and polymerized at 60°C for 48 hr. Sections were cut with an LKB Nova ultramicrotome and collected on copper grids and stained with uranyl acetate and lead citrate. Preparations were observed and photographed with a Philips CM10 electron microscope.

Immunoelectron Microscopy of Testes and Embryos

2–3 hr embryos overexpressing GFP-DSAS-6 were dechorionated in freshly made bleach solution and washed with distilled water. The vitteline membrane was removed in 1:1 solution of 25% paraformaldehyde and heptane for 3 min with strong agitation. Testes from *pUbq-GFP-DSAS-6* third instar larvae and pupae were dissected in PBS. Devitellinized embryos and testes were fixed for 10 min in 1% paraformaldehyde and 0.5% Triton-X. Samples were cut longitudinally and incubated 1 hr at room temperature in PBS with 0.1% BSA. GFP-DSAS-6 was localized in embryos and testes after incubation overnight at 4°C with an antibody against GFP. Samples were then incubated for 1 hr with secondary antibodies coupled to 5 nm gold particles (BioCell, Cardiff), diluted 1:25. Samples were fixed overnight in a solution of 2.5% glutaraldehyde in PBS and postfixed for 1 hr in osmium tetroxide and processed as above for embedding in Epon-Araldite and sectioning. Controls were performed with omission of primary antibody.

Sequence Analysis

We used PSI-Blast [S14] to search for SAS-6 homologs in GenBank. The PISA domain, a SAS-6-specific domain [S15], which extends from residues 39 to 91 in the human sequence, was used as query sequence. Two iterations were sufficient to identify homologs in the model organisms we choose to investigate in this study, except for *C. reinhardtii*, which is not in GenBank. As such, the *C. reinhardtii* homolog was obtained by querying this genome at http://genome.jgi-psf.org/Chlre3/Chlre3.home.html, via BlastP [S16, S17]. All the identified proteins are reciprocal best hits for this domain, suggesting that they are orthologous. Sequence alignments were performed with MUSCLE version 3.6 [S18] and phylogenetic reconstruction was done by maximum likelihood [S19] with the JTT model for amino acid substitution [S20], implemented in PHYLIP [S21]. The bootstrap values were calculated generating 100 replicates and a consensus tree constructed.

Supplemental References

S1. Thibault, S.T., Singer, M.A., Miyazaki, W.Y., Milash, B., Dompe, N.A., Singh, C.M., Buchholz, R., Demsky, M., Fawcett, R., Francis-Lang, H.L., et al. (2004). A complementary transposon tool kit for *Drosophila melanogaster* using P and piggyBac. Nat. Genet. *36*, 283–287.

S2. Martinez-Campos, M., Basto, R., Baker, J., Kernan, M., and Raff, J.W. (2004). The *Drosophila* pericentrin-like protein is essential for cilia/flagella function, but appears to be dispensable for mitosis. J. Cell Biol. *165*, 673–683.

S3. Bettencourt-Dias, M., Sinka, R., Frenz, L., and Glover, D.M. (2004). RNAi in *Drosophila* cell cultures. In Gene Silencing by RNA Interference: Technology and Application, M. Sohail, ed. (Boca Raton, FL: CRC Press), pp. 147–165.

S4. Bettencourt-Dias, M., Rodrigues-Martins, A., Carpenter, L., Riparbelli, M., Lehmann, L., Gatt, M.K., Carmo, N., Balloux, F., Callaini, G., and Glover, D.M. (2005). SAK/PLK4 is required for centriole duplication and flagella development. Curr. Biol. *15*, 2199–2207.

S5. Bettencourt-Dias, M., Giet, R., Sinka, R., Mazumdar, A., Lock, W.G., Balloux, F., Zafiropoulos, P.J., Yamaguchi, S., Winter, S., Carthew, R.W., et al. (2004). Genome-wide survey of protein kinases required for cell cycle progression. Nature *432*, 980–987.

S6. Basto, R., Lau, J., Vinogradova, T., Gardiol, A., Woods, C.G., Khodjakov, A., and Raff, J.W. (2006). Flies without centrioles. Cell *125*, 1375–1386.

S7. Rodrigues-Martins, A., Riparbelli, M., Callaini, G., Glover, D.M., and Bettencourt-Dias, M. (2007). Revisiting the role of the mother centriole in centriole biogenesis. Science *316*, 1046–1050.

S8. Cenci, G., Bonaccorsi, S., Pisano, C., Verni, F., and Gatti, M. (1994). Chromatin and microtubule organization during premeiotic, meiotic and early postmeiotic stages of *Drosophila melanogaster* spermatogenesis. J. Cell Sci. *107*, 3521–3534.

S9. Barbosa, V., Yamamoto, R.R., Henderson, D.S., and Glover, D.M. (2000). Mutation of a *Drosophila* gamma tubulin ring complex subunit encoded by discs degenerate-4 differentially disrupts centrosomal protein localization. Genes Dev. *14*, 3126–3139.

S10. Donaldson, M.M., Tavares, A.A., Ohkura, H., Deak, P., and Glover, D.M. (2001). Metaphase arrest with centromere separation in polo mutants of *Drosophila*. J. Cell Biol. *153*, 663–676.

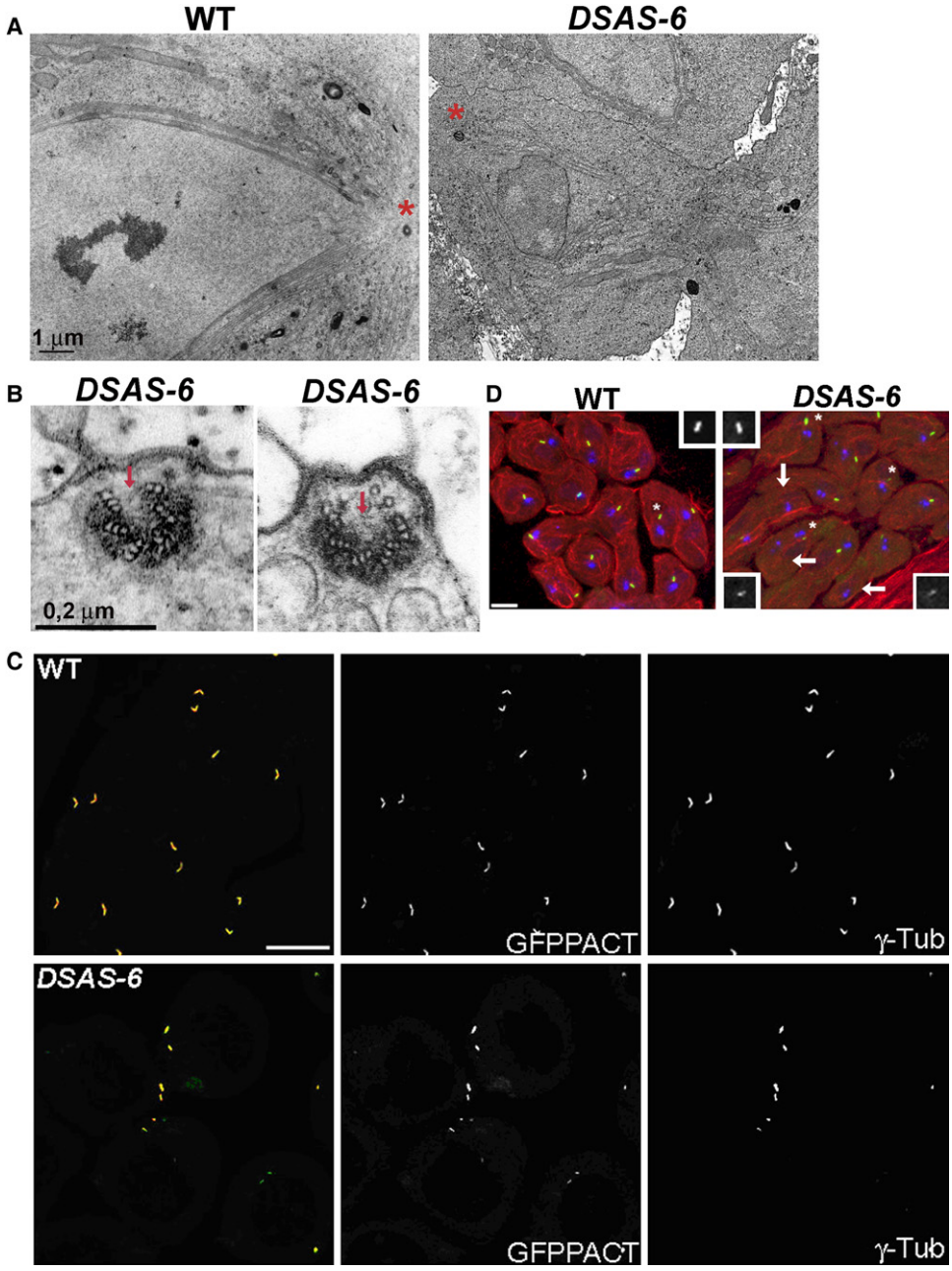

Figure S5. DSAS-6 Is Involved in Centriole Assembly

(A) Absence of centrioles at the poles of a meiosis I spindle in *DSAS-6* mutant primary spermatocytes as observed by TEM. Note that wild-type (WT) cell is in prometaphase while mutant is in telophase. Asterisks show poles of meiotic spindle.

(B) Structurally incomplete centrioles observed in *DSAS-6* mutant primary spermatocytes by TEM, two serial sections. Arrows indicate absence of triplets. Scale bar as indicated.

(C) Small centrioles observed in *DSAS-6* mutant primary spermatocytes in G2 observed by both GFP-PACT and γ-tubulin staining. At this stage of development, γ-tubulin labels exclusively the centrioles as there is very little PCM [S4]. Note that these two markers colocalize and show smaller centrioles. GFP-PACT (green), γ-tubulin (red). Scale bar represents 10 μm.

(D) *DSAS6* mutant spermatids do not show more than one single GFP-PACT body. Analysis of Nebenkern-stage cells showed only one GFP-PACT dot per cell in both wild-type and *DSAS-6* mutant. If centrioles were unstable and were to fragment in the *DSAS-6* mutant, we would expect to see cells with more than one GFP-PACT body, which was not the case. Insets correspond to 2× magnification of centrioles in *DSAS-6* mutant (GFP-PACT channel). α-tubulin (red), GFP-PACT (green), DNA (blue). Arrows indicate cells without visible centrioles. Scale bar represents 10 μm.

S11. Warn, R.M., and Warn, A. (1986). Microtubule arrays present during the syncytial and cellular blastoderm stages of the early *Drosophila* embryo. Exp. Cell Res. *163*, 201–210.

S12. Riparbelli, M.G., Massarelli, C., Robbins, L.G., and Callaini, G. (2004). The abnormal spindle protein is required for germ cell mitosis and oocyte differentiation during *Drosophila* oogenesis. Exp. Cell Res. *298*, 96–106.

S13. Tavosanis, G., Llamazares, S., Goulielmos, G., and Gonzalez, C. (1997). Essential role for gamma-tubulin in the acentriolar female meiotic spindle of *Drosophila*. EMBO J. *16*, 1809–1819.

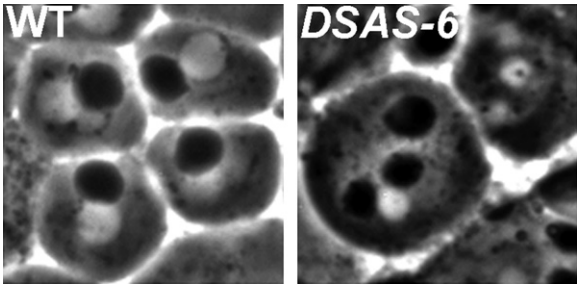

Figure S6. *DSAS-6* Mutant Spermatids Show Irregular Numbers of Nuclei and Nebenkern

Phase-contrast images of spermatids showing irregular ratio of nuclei to Nebenkern in *DSAS-6* mutant testes. Note that in the WT there is always a 1:1 ratio.

S14. Altschul, S.F., Madden, T.L., Schaffer, A.A., Zhang, J., Zhang, Z., Miller, W., and Lipman, D.J. (1997). Gapped BLAST and PSI-BLAST: a new generation of protein database search programs. Nucleic Acids Res. *25*, 3389–3402.

S15. Leidel, S., Delattre, M., Cerutti, L., Baumer, K., and Gonczy, P. (2005). SAS-6 defines a protein family required for centrosome duplication in *C. elegans* and in human cells. Nat. Cell Biol. *7*, 115–125.

S16. Altschul, S.F., Gish, W., Miller, W., Myers, E.W., and Lipman, D.J. (1990). Basic local alignment search tool. J. Mol. Biol. *215*, 403–410.

S17. Gish, W., and States, D.J. (1993). Identification of protein coding regions by database similarity search. Nat. Genet. *3*, 266–272.

S18. Edgar, R.C. (2004). MUSCLE: multiple sequence alignment with high accuracy and high throughput. Nucleic Acids Res. *32*, 1792–1797.

S19. Felsenstein, J. (1981). Evolutionary trees from DNA sequences: a maximum likelihood approach. J. Mol. Evol. *17*, 368–376.

S20. Jones, D.T., Taylor, W.R., and Thornton, J.M. (1992). The rapid generation of mutation data matrices from protein sequences. Comput. Appl. Biosci. *8*, 275–282.

S21. Felsenstein, J. (1993). PHYLIP: phylogenetic inference package, Version 3.5 (Seattle: University of Washington Department of Genetics).

S22. Pelletier, L., Ozlu, N., Hannak, E., Cowan, C., Habermann, B., Ruer, M., Muller-Reichert, T., and Hyman, A.A. (2004). The *Caenorhabditis elegans* centrosomal protein SPD-2 is required for both pericentriolar material recruitment and centriole duplication. Curr. Biol. *14*, 863–873.

S23. Kemp, C.A., Kopish, K.R., Zipperlen, P., Ahringer, J., and O'Connell, K.F. (2004). Centrosome maturation and duplication in *C. elegans* require the coiled-coil protein SPD-2. Dev. Cell *6*, 511–523.

S24. Goshima, G., Wollman, R., Goodwin, S.S., Zhang, N., Scholey, J.M., Vale, R.D., and Stuurman, N. (2007). Genes required for mitotic spindle assembly in *Drosophila* S2 cells. Science *316*, 417–421.

S25. Dippell, R.V. (1968). The development of basal bodies in paramecium. Proc. Natl. Acad. Sci. USA *61*, 461–468.

S26. Dirksen, E.R. (1971). Centriole morphogenesis in developing ciliated epithelium of the mouse oviduct. J. Cell Biol. *51*, 286–302.

S27. Dawe, H.R., Farr, H., and Gull, K. (2007). Centriole/basal body morphogenesis and migration during ciliogenesis in animal cells. J. Cell Sci. *120*, 7–15.

S28. Raff, E.C., Hutchens, J.A., Hoyle, H.D., Nielsen, M.G., and Turner, F.R. (2000). Conserved axoneme symmetry altered by a component beta-tubulin. Curr. Biol. *10*, 1391–1394.

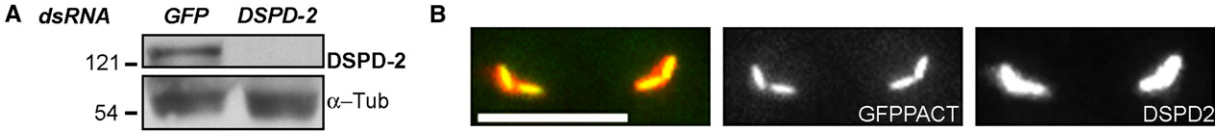

Figure S7. DSPD-2 Antibody Specificity and Localization to Centrioles

(A) RNAi against *DSPD-2* reduces the amount of endogenous DSPD-2 protein in S2 cells as detected by western with an antibody against SPD-2 made by us (see Experimental Procedures).

(B) DSPD-2 antibody recognizes the centrioles in the 16 cell cysts in G2, because the signal colocalizes with the centriolar marker GFP-PACT. DSPD-2 (red), GFP-PACT (green). Scale bar represents 5 μm [S22–S24]

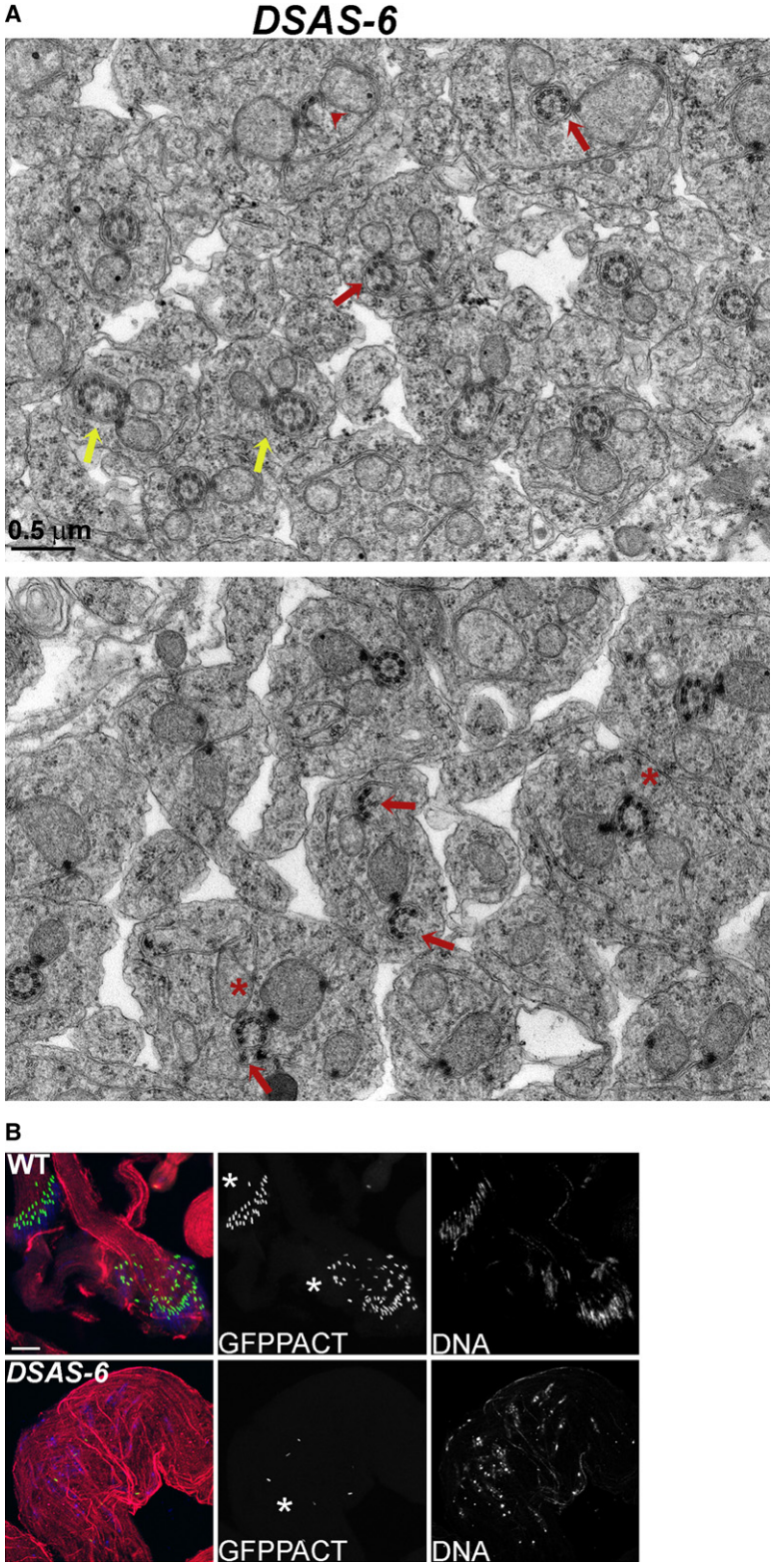

Figure S8. Structurally Abnormal Flagella and Axonemes in *DSAS-6* Mutants

(A) Examples of structural abnormalities observed in the axoneme of *DSAS-6* mutant spermatids by TEM. Red arrows indicate fewer doublets. Asterisks indicate the absence of central pair. Yellow arrows indicate axonemes with more than nine doublets. Arrowhead shows open axoneme structure. Scale bar as indicated.

(B) *DSAS-6* mutants showed disorganized spermatids with reduced number of basal bodies. Asterisks indicate basal bodies. α-tubulin (red), GFP-PACT (green), DNA (blue). Scale bar represents 10 μm.

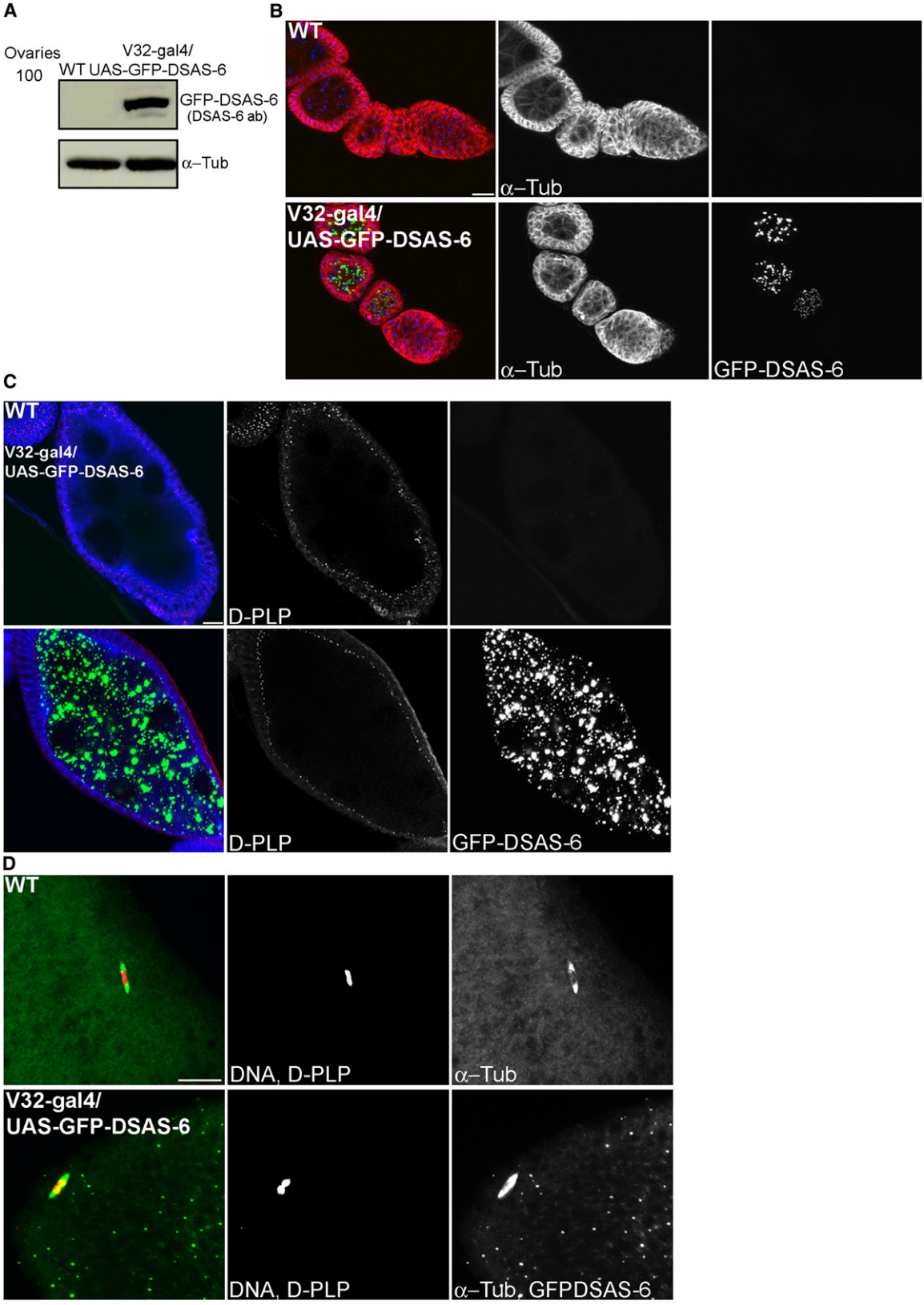

Figure S9. No Extra MTOCs Are Detected during Oogenesis and Meiosis I in Females Overexpressing GFP-DSAS-6 in the Germline

(A) Overexpression of *UAS-GFP-DSAS-6* in ovaries with the maternal driver *V32-gal4*.

(B) GFP-DSAS-6 overexpression is detected at the end of stage 2 of oogenesis, with no free asters being formed at this stage. GFP-DSAS-6 (green), α-tubulin (red), DNA (blue). Scale bar represents 50 μm.

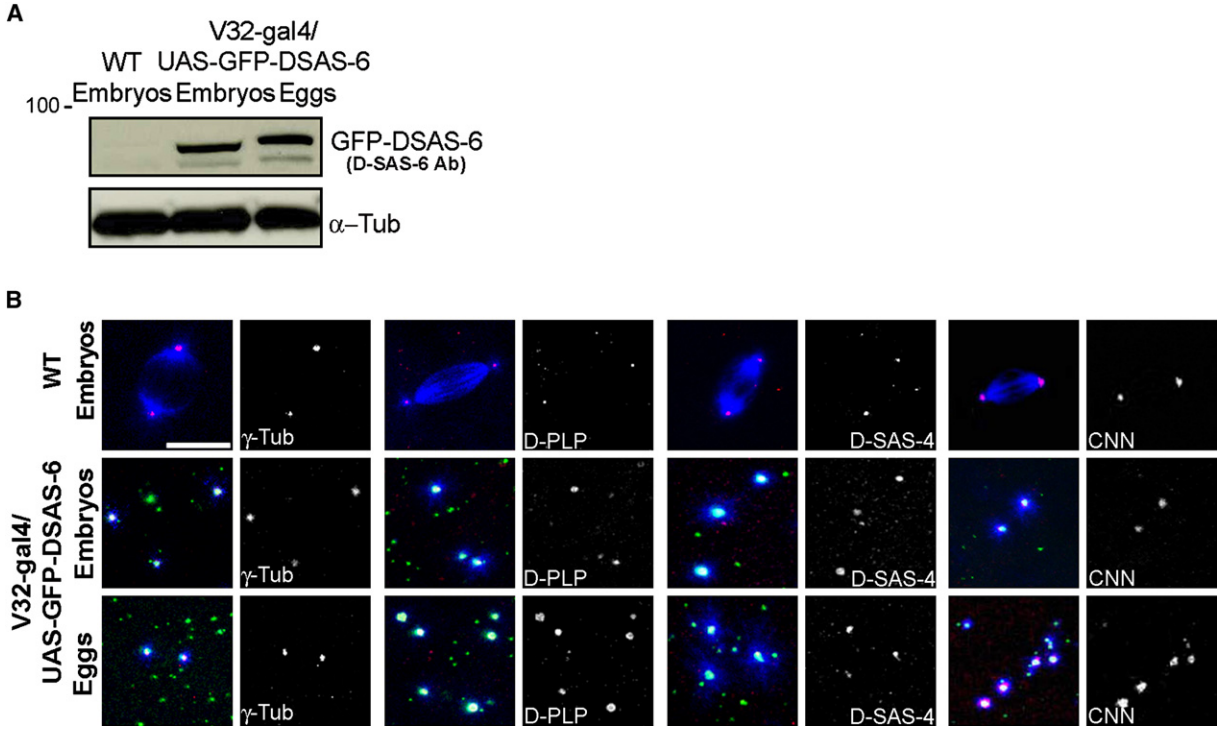

Figure S10. Overexpression of GFP-DSAS-6 Generates Free Asters in Both Embryos and Eggs

(A) Overexpression of *UASp-GFP-DSAS-6* in embryos and unfertilized eggs by the maternal driver *V32-gal4*.

(B) The free asters show PCM (D-PLP, γ-Tub, CNN) and centriole markers (D-PLP, DSAS-4) in both embryos and eggs from mothers overexpressing GFP-DSAS-6 in the germline. Note that microtubules colocalize with GFP-DSAS-6 only when those markers were present. γ-tubulin (red), D-PLP (red), DSAS-4 (red), CNN (red), GFP-DSAS-6 (green), α-tubulin (blue). Scale bar represents 10 μm.

(C) No D-PLP containing structures are present in the germ cells in late oogenesis despite the large amount of GFP-DSAS-6 protein aggregates. These may result from aggregation of DSAS-6, because of its coiled-coil domain. D-PLP (red), GFP-DSAS-6 (green), α-tubulin (blue). Scale bar represents 10 μm.

(D) Meiosis I occurs normally in eggs from *V32-gal4/UAS-GFP-DSAS-6* females (overexpressing DSAS-6). Note that there are no extra D-PLP bodies. D-PLP (red), DNA (red), GFP-DSAS-6 (green), α-tubulin (green). Scale bar represents 10 μm.

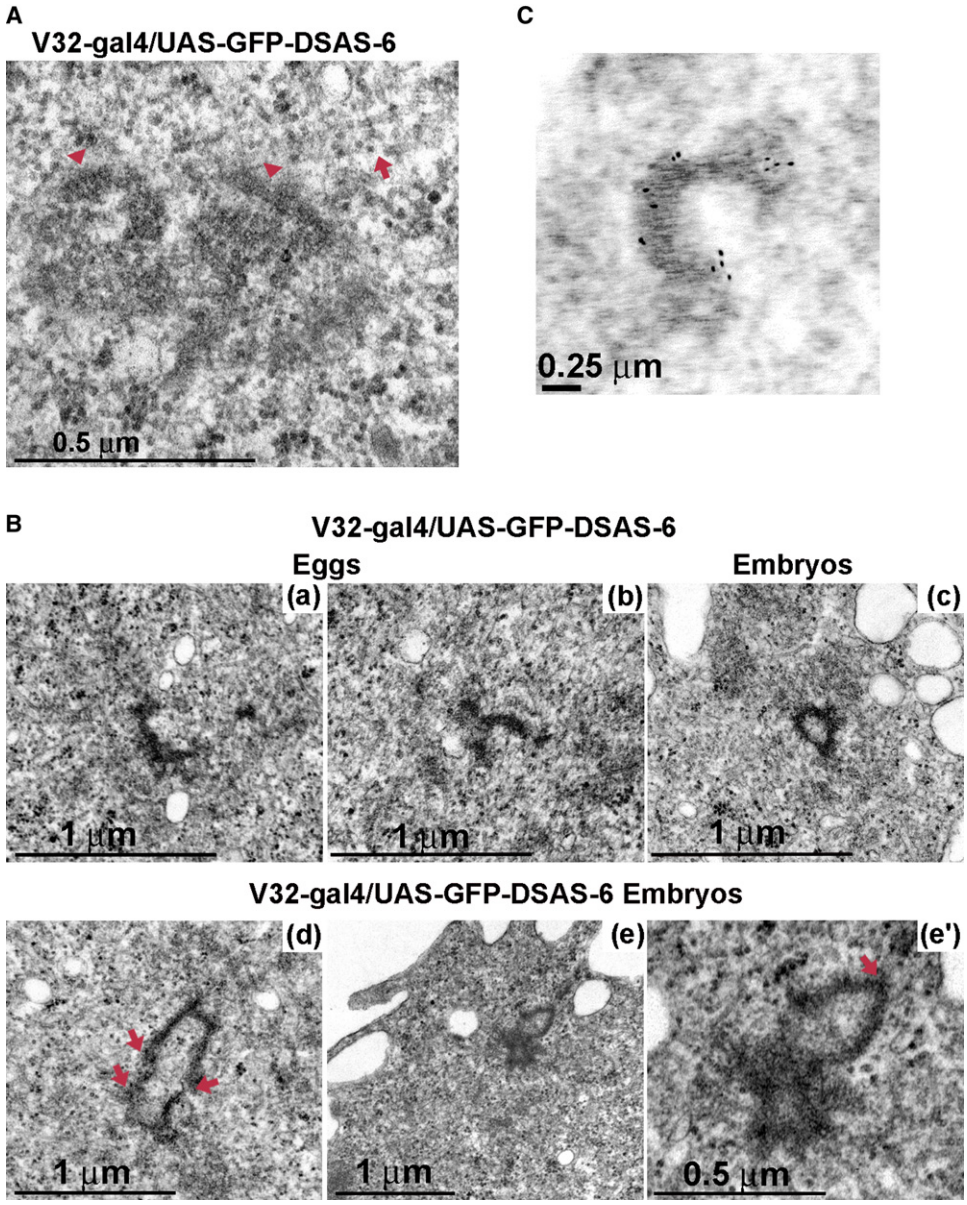

Figure S11. Overexpression of DSAS-6 in Unfertilized and Fertilized Eggs Leads to the Formation of Tube-like Structures

(A) Microtubules (arrow) and PCM (arrowheads) are observed in embryos overexpressing GFP-DSAS-6.

(B) GFP-DSAS-6 overexpression leads to the formation of tube-like structures in both eggs (a, b) and embryos (c, d, e, e′). Tubes formed were 2.2× bigger in diameter on average as compared to wild-type centrioles. We measured the largest internal diameter in all tubes where such measurement was applicable. Note that in general they were not perfect circles and some show wrong orientation of circle (arrows).

(C) Immunoelectron microscopy shows that DSAS-6 localizes to the tube formed by overexpression of GFP-DSAS-6. Scale bar as indicated.

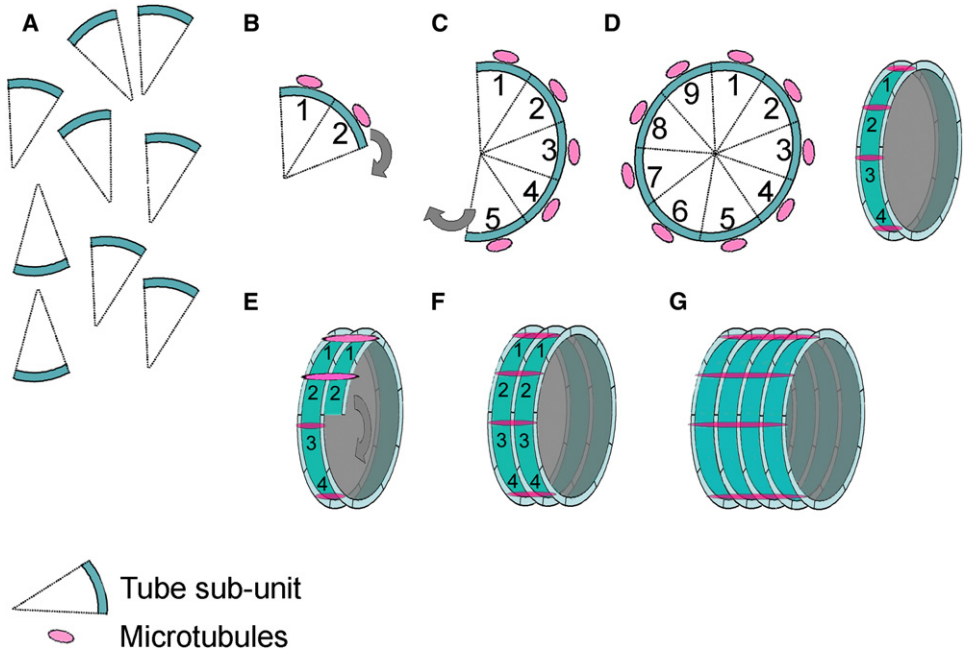

Figure S12. Centriole Assembly and Elongation Is Modular

Our data suggest that DSAS-6 promotes the assembly of a centriolar scaffold, a tube, which is composed of nine modular units.

(A) We suggest that these units have left-right, top-down polarity (not represented here), thereby ensuring the correct binding. This polarity could be provided by different molecules in each side of the unit. Their selective interaction could provide specificity in unit binding. Short of experimental evidence, the unit is depicted here as a triangle but it could just as well be a ninth of the circle.

(B–D) We suggest that units attach to each other sequentially, one by one, in order to form the tube. These structures can recruit centriole microtubules (pink). Note that in (D), a disc of the tube is represented in cross section (left) and in transversal section (right).

(E–G) We propose that centriole elongation occurs by adding more units, one by one, on top of the previous "disc." It is possible that this tube is disassembled after the centriole is completely built.

It is not clear what the relation might be between the tube observed here and the structures previously described to be involved in centriole/basal body biogenesis: the generative disk and self-assembling cartwheel structures [S25], or even the deuterosome, an amorphous electron-dense disk, shown to be involved in basal body biogenesis in ciliated tissues (reviewed in [S26, S27]). It will be important in the future to characterize those structures further with molecular markers in order to understand the relationship between them.

This model explains our following results.

(1) We have never observed missing triplets/doublets that are not contiguous in the centriolar/axoneme circle, i.e., more than one "block" of missing doublets (Figures 1E and 3; Figures S5B and S8A). The most commonly observed incomplete centrioles and axonemes in the mutants were missing 1 to 5 adjacent triplets/doublets of microtubules (Figures 1E and 3; Figures S5 and S8). This suggests that the unit for the construction of the tube is one ninth of it.

(2) Elongation problems observed in *DSAS-6* mutants (Figures 1D and 1G) could be accounted for if some discs at the bottom were able to form but overlaying ones were not completed. If DSAS-6 regulates the binding of subunits (horizontally and longitudinally), we would expect that its absence could lead to changes in orientation of PCM and microtubules (Figure 1F) and to missing triplets as we described.

(3) DSAS-6 overexpression could lead to incorrect binding of the modules and as such the formation of ectopic tubes of abnormal orientation and abnormal size (Figure 4B; Figure S11). In fact, the tubes formed were on average 2.2× bigger in diameter than wild-type centrioles. This increase in size could be due to an excess of DSAS-6 in relation to other molecules that regulate centriole biogenesis. This excess could catalyze the formation of larger tubes by promoting the binding of supernumerary units, some of them in the wrong orientation. The latter could give rise to the appearance of several open circles bound to each other (Figure 4B; Figure S11).

(4) The origin of excessive doublets in 9% of mutant axonemes (Figure 3; Figure S8) is not clear at the moment. It will be important to clarify whether they arose from centrioles with extra triplets or, alternatively, extra doublets were only inserted half way through the axoneme length as a consequence of other problems in axoneme structure [S28].

Blue structures, tube subunits/module; pink structures, MT triplets.